Biogeosciences, 6, 585–599, 2009
www.biogeosciences.net/6/585/2009/

Biogeosciences

An empirical model simulating diurnal and seasonal CO_2 flux for diverse vegetation types and climate conditions

M. Saito[1], **S. Maksyutov**[1], **R. Hirata**[2], **and A. D. Richardson**[3]

[1]Center for Global Environmental Research, National Institute for Environmental Studies, Tsukuba 305-8506, Japan
[2]National Institute for Agro-Environmental Sciences, Tsukuba 305-8604, Japan
[3]Complex Systems Research Center, University of New Hampshire, Durham, NH 03824, USA

Received: 27 August 2008 – Published in Biogeosciences Discuss.: 9 October 2008
Revised: 11 March 2009 – Accepted: 24 March 2009 – Published: 16 April 2009

Abstract. We present an empirical model for the estimation of diurnal variability in net ecosystem CO_2 exchange (NEE) in various biomes. The model is based on the use of a simple saturated function for photosynthetic response of the canopy, and was constructed using the AmeriFlux network dataset that contains continuous eddy covariance CO_2 flux data obtained at 24 ecosystems sites from seven biomes. The physiological parameters of maximum CO_2 uptake rate by the canopy and ecosystem respiration have biome-specific responses to environmental variables. The model uses simplified empirical expression of seasonal variability in biome-specific physiological parameters based on air temperature, vapor pressure deficit, and annual precipitation. The model was validated using measurements of NEE derived from 10 AmeriFlux and four AsiaFlux ecosystem sites. The predicted NEE had reasonable magnitude and seasonal variation and gave adequate timing for the beginning and end of the growing season; the model explained 83–95% and 76–89% of the observed diurnal variations in NEE for the AmeriFlux and AsiaFlux ecosystem sites used for validation, respectively. The model however worked less satisfactorily in two deciduous broadleaf forests, a grassland, a savanna, and a tundra ecosystem sites where leaf area index changed rapidly. These results suggest that including additional plant physiological parameters may improve the model simulation performance in various areas of biomes.

1 Introduction

Simulation of atmospheric CO_2 variability by atmospheric transport modeling depends critically on the use of terrestrial ecosystem models to accurately simulate diurnal and seasonal variations in terrestrial biospheric processes. Comparisons of seasonal cycles and their amplitudes between observed atmospheric CO_2 variability and that simulated by several terrestrial ecosystem models based on simplified assumptions of biospheric processes have often shown poor agreement (e.g., Nemry et al., 1999). Often model parameter adjustment is necessary to improve fit with the atmospheric observations. Fung et al. (1987), for example, adjusted the seasonal cycle amplitude by modifying the value of the Q_{10} temperature coefficient for ecosystem respiration.

Successful simulations of seasonal cycle have been made with more recent and sophisticated models, e.g., CASA (Potter et al., 1993; Randerson et al., 1997). Process-based models differ in their parameterization of primary production. Models based on light-use efficiency, such as CASA and TURC (Ruimy et al., 1996), assume a linear relationship between monthly net primary production (NPP) and monthly solar radiation (Monteith, 1972) that is limited by water availability and temperature. Although these models appear to be successful in seasonal cycle simulation as a whole, their extension to cover diurnal cycles should be accompanied by the introduction of a more realistic, non-linear relationship between CO_2 uptake by terrestrial vegetation and solar radiation at an hourly time scale. The biochemical model proposed by Farquhar et al. (1980) describes the dependence of photosynthesis on solar radiation, with CO_2 uptake rate limited by maximum photosynthetic capacity. This concept is used widely in land-surface schemes for meteorology and hydrology, such as SiB (Sellers et al., 1986) and LSM (Bonan, 1996, 1998), but is less successful in carbon cycle studies because of a lack of empirical data or models for describing the seasonal and spatial variability of the necessary parameters, such as maximum photosynthetic capacity. Alternative ways of evaluating biospheric processes are therefore required for the estimation of diurnal cycles in CO_2 variability. In some

Correspondence to: M. Saito
(saito.makoto@nies.go.jp)

cases, empirical models can fit the data more closely than mechanistic models (Thornley, 2002).

For studies of the diurnal cycle of CO_2 variability, long-term field measurement studies using the eddy covariance method have been conducted in recent years at many sites, covering various ecosystems around the world (Baldocchi, 2008). These sites are now organized into a global network, FLUXNET, and a large body of observation data is being accumulated. The eddy covariance method routinely provides direct measurements of net ecosystem CO_2 exchange (NEE) between the atmosphere and the biosphere. The data obtained from these field measurements can be useful, especially for constructing models to predict the diurnal cycle of CO_2 variability associated with biospheric processes, since they provide direct information on turbulence and scalar fluctuations at time scales from seconds to hours over the local vegetation canopy.

In the present work, our focus is on constructing a model that simulates the diurnal variability of NEE in various ecosystems based solely on environmental forces. For this work, we used data from the AmeriFlux and AsiaFlux networks.

2 Materials and methods

2.1 Input data

All half-hourly or hourly CO_2 flux data used were obtained from the AmeriFlux network (Hargrove et al., 2003). Sixty-two years' worth of eddy covariance flux data taken from 24 AmeriFlux ecosystem sites and covering seven major biomes in the latitudes from Alaska to Brazil were analyzed. The biomes consisted of six evergreen needle-leaf forests (ENF), two evergreen broadleaf forests (EBF), four deciduous broadleaf forests (DBF), four mixed forests (MF), three grasslands (GRS), two savannas (SVN), and three tundra ecosystems (TND) (Table 1). Each site was equipped with an eddy covariance system consisting of an open- or closed-path infrared gas analyzer and a three-dimensional sonic anemometer/thermometer. AmeriFlux Level 2 products, which contain non-gap-filled CO_2 flux data, were used as input data to avoid contamination associated with gap-filling procedures. The periods analyzed for each ecosystem site are listed in Table 1.

Half-hourly or hourly air temperature (°C), vapor pressure deficit (VPD; kPa), incident photosynthetic photon flux density (PPFD; μmol photon m^{-2} s^{-1}), and precipitation (mm) for individual sites were also obtained from the AmeriFlux network. For all sites, air temperature and precipitation data that were missing because of instrument malfunction were filled using the Global Surface Summary of Day (GSOD) data sets to compute annual mean temperature and annual precipitation. The GSOD is a product of the Integrated Surface Data provided by the National Climate Data Center, and includes 13 daily summary parameters over 9000 global stations.

2.2 Modeling approach

To predict vegetation photosynthesis and its light response, a nonrectangular hyperbolic model:

$$\mathrm{NEE}=\frac{1}{2\theta}\left(\alpha Q+P_{\max}-\sqrt{(\alpha Q+P_{\max})^2-4\alpha\theta Q P_{\max}}\right)-\mathrm{RE} \quad (1)$$

has been widely applied (e.g., Rabinowitch, 1951; Peat, 1970), where α is the initial slope of the light response curve and an approximation of the canopy light utilization efficiency (μmol CO_2 (μmol photon)$^{-1}$), $P_{\max}$ is the maximum CO_2 uptake rate of the canopy (μmol CO_2 m^{-2} s^{-1}), RE is the average daytime ecosystem respiration (μmol CO_2 m^{-2} s^{-1}), θ is a curvature parameter, and Q is PPFD. Johnson and Thornley (1984) have shown that a nonrectangular hyperbola predicts the integrated daily canopy photosynthesis with an accuracy better than 1% when it is averaged over various irradiances. More recently, this hyperbola has been successfully used in the gap-filling method to obtain continuous eddy covariance CO_2 fluxes over a year, and to estimate the total annual carbon budget over various biomes (e.g., Gilmanov et al., 2003; Hirata et al., 2008).

Here, we derive a simple and empirical model for predicting the diurnal variability in NEE over a number of biomes on the basis of the nonrectangular hyperbolic model. To apply the nonrectangular hyperbola, the unknown number parameters (α, $P_{\max}$, and RE in Eq. (1)) have to be determined, whereas θ is fixed at 0.9 following Kosugi et al. (2005) and Saigusa et al. (2008). To formulate individual unknown parameters, we first calculated the seasonal course of those parameters for every site listed in Table 1 by using all available daytime data. The values of parameters were estimated for each day by fitting the data to Eq. (1) using the least-squares method. To reduce poor fitting of Eq. (1) that results from the limited availability and noise in CO_2 flux data, the parameters for each day were estimated using a 15-day moving window. Individual parameters exhibited seasonal variations, and the variability and amplitude of individual parameters clearly differed among the ecosystem sites and biomes measured. Below we describe how we formulated the seasonal courses of three unknown parameters for each biome.

The seasonal course of $P_{\max}$ was correlated with those of temperature and VPD for each biome, and the strength of the correlations with these environmental factors differed among biomes. Figure 1 shows the normalized $P_{\max}$ under different daily mean air temperatures T_a (°C) and VPD_a (kPa) averaged over a 15-day period, consistent with that used in the fitting of Eq. (1). The value of $P_{\max}$ was normalized by the maximum $P_{\max}$ at the site over the entire period analyzed. The largest values of the normalized $P_{\max}$ occurred in each biome, except for TND, when T_a was approximately between 20°C and 25°C, and VPD_a was lower than 1 kPa. Although scatter exists, the normalized $P_{\max}$ for each biome decreased with decreasing T_a and increasing VPD_a. On the basis of the

Table 1. List of AmeriFlux eddy covariance measurement sites analyzed in this study. Annual mean temperature (AMT) and annual precipitation (AP) are mean values for the period indicated.

Site, country	Year	Latitude, longitude	AMT (°C)	AP (mm)	Reference
Evergreen needle leaf forest (ENF)					
UCI-1930 burn site, Canada	2002–2004	55.91° N, 98.53° W	−2.7	412	Wang et al. (2003)
UCI-1850 burn site, Canada	2002–2004	55.88° N, 98.48° W	−2.7	412	McMillan et al. (2008)
Duke Forest loblolly pine, USA	2002–2004	35.98° N, 79.09° W	17.3	1140	Katul et al. (1999)
Howland forest, USA	2002–2004	45.20° N, 68.74° W	6.8	836	Hollinger et al. (2004)
Metolius, USA	2004–2005	44.45° N, 121.56° W	9.1	405	Schwarz et al. (2004)
Slashpine-Donaldson, USA	2002–2004	29.76° N, 82.16° W	20.4	1072	Gholz and Clark (2002)
Evergreen broadleaf forest (EBF)					
Santarem-Km67-Primary Forest, Brazil	2002–2004	2.86° S, 54.96° W	25.3	1591	Martens et al. (2004)
Florida-Kennedy Space Center, USA	2004–2006	28.61° N, 80.67° W	21.6	1123	Dore et al. (2003)
Deciduous broadleaf forest (DBF)					
Duke Forest hardwoods, USA	2003–2005	35.97° N, 79.10° W	15.1	1091	Katul et al. (2003)
Harvard Forest EMS Tower, USA	2001–2003	42.54° N, 72.17° W	7.5	1023	Goulden et al. (1996)
Missouri Ozark Site, USA	2005–2006	38.74° N, 92.20° W	13.5	878	Gu et al. (2006)
Bartlett Experimental Forest, USA	2004–2005	44.07° N, 71.29° W	7.1	1402	Jenkins et al. (2007)
Mixed forest (MF)					
Intermediate hardwood, USA	2003	46.73° N, 91.23° W	5.3	625	–
Mature red pine, USA	2003–2005	46.74° N, 91.17° W	5.6	706	–
Mixed young jack pine, USA	2004	46.65° N, 91.09° W	5.0	649	–
Park Falls/WLEF, USA	1997, 1999	45.95° N, 90.27° W	5.2	842	Yi et al. (2001)
Grassland (GRS)					
Duke Forest open field, USA	2003–2004	35.97° N, 79.09° W	14.9	1144	Katul et al. (2003)
Brookings, USA	2005–2006	44.35° N, 96.84° W	7.2	608	Gilmanov et al. (2005)
Walnut River Watershed, USA	2002–2004	37.52° N, 96.86° W	13.7	1046	LeMone et al. (2002)
Savanna (SVN)					
Santa Rita Mesquite, USA	2004–2006	31.82° N, 110.87° W	19.1	303	Scott et al. (2008)
Audubon Research Ranch, USA	2004–2006	31.59° N, 110.51° W	15.8	361	–
Tundra (TND)					
Atqasuk, USA	2004–2006	70.47° N, 157.41° W	−10.6	108	–
Barrow, USA	2000–2002	71.32° N, 156.63° W	−11.3	172	Eugster et al. (2000)
Ivotuk, USA	2004–2006	68.49° N, 155.75° W	−9.3	241	Epstein et al. (2004)

variability in the normalized $P_{\max}$ shown in Fig. 1, and in the interest of reducing the number of parameters and using meteorological data that were readily available everywhere, we expressed $P_{\max}$ as a function of the environmental variables of air temperature and VPD as follows:

$$P_{\max} = P_{\max}^{\mathrm{PM}} \cdot F_T \cdot F_V \tag{2}$$

where $P_{\max}^{\mathrm{PM}}$ is the potential maximum value of $P_{\max}$ under unstressed conditions, and F_T and F_V denote the coefficient functions for air temperature and VPD, respectively. We used the following equations to express F_T and F_V, respectively:

$$F_T = \frac{(T_a - T_{\max})(T_a - T_{\mathrm{mim}})}{(T_a - T_{\max})\,(T_{\mathrm{a}} - T_{\mathrm{mim}}) - (T_a - T_{\mathrm{opt}})^2} \tag{3}$$

$$F_V = \left[\frac{1}{1 + (\mathrm{VPD}_a / a_{\mathrm{FV}})^{b_{\mathrm{FV}}}}\right] \tag{4}$$

where $T_{\max}$, $T_{\min}$, and T_{opt} are the maximum, minimum, and optimum temperatures (°C), respectively, for photosynthesis, and a_{FV} (kPa) and b_{FV} are constant coefficients. a_{FV} is the value of VPD when F_V=0.5. The parameter values of $T_{\max}$,

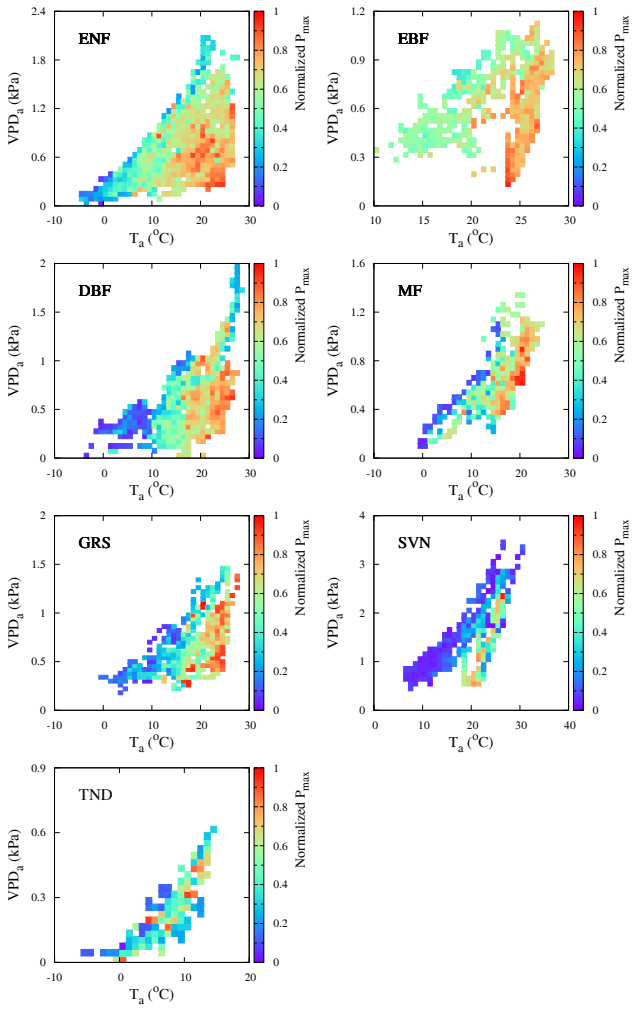

Fig. 1. Dependence of normalized P_{max} on daily mean air temperature (T_a; °C) and vapor pressure deficit (VPD_a; kPa) over 15-day periods for seven biomes. The daily values of P_{max} were normalized by the maximum P_{max} at the site, and were then aggregated for each biome. The normalized values of P_{max} in each grid are averages corresponding to the range of T_a and VPD_a, and the magnitudes of these are represented in color.

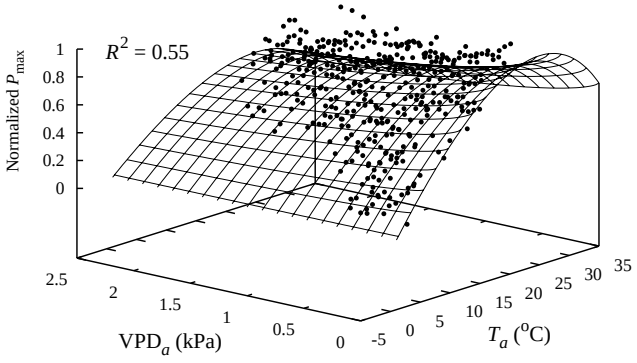

Fig. 2. Normalized P_{max} in evergreen needle-leaf forests (ENF) under different conditions of T_a (°C) and VPD_a (kPa). The solid circles corresponds to grids shown in Fig. 1, and the response surface fit of Eqs. (3) and (4) using the nonlinear least squares method.

T_{min}, T_{opt}, a_{FV}, and b_{FV} were determined for each biome by fitting the normalized P_{max} to Eqs. (3) and (4) using the nonlinear least-squares method (Table 2). An example of the fitting is shown in Fig. 2 for ENFs.

To formulate P_{max}^{PM} in Eq. (2), all daily P_{max} obtained by fitting Eq. (1) with observed CO_2 flux data were divided by F_T and F_V, and then the annual maximum value of unstressed P_{max} was selected for each ecosystem site from among the data observed under conditions when T_a was ±5°C in T_{opt}. To avoid uncertainty in the value of P_{max} due to random flux measurement error, a computed unstressed maximum P_{max} was averaged for the 7-day period around the maximum day. This value was defined as P_{max}^{PM}. Next, P_{max}^{PM} was approximated as a function of annual NPP, assuming that the maximum value of P_{max} was proportional to the annual NPP. Annual NPP (g C m^{-2} y^{-1}) for each site was estimated using the Miami model (Lieth, 1975), as follows:

$$\begin{aligned} \mathrm{NPP(AMT,\ AP)} &= \min\{\mathrm{NPP}_T\mathrm{(AMT)},\ \mathrm{NPP}_h\mathrm{(AP)}\}; \\ \mathrm{NPP}_T\mathrm{(AMT)} &= \frac{1350}{1+\exp(1.315-0.119\cdot\mathrm{AMT})}, \\ \mathrm{NPP}_h\mathrm{(AP)} &= 1350(1-\exp(-0.000664\cdot\mathrm{AP})) \end{aligned} \quad (5)$$

where AMT is annual mean temperature (°C) and AP is annual precipitation (mm). The unstressed maximum P_{max} (i.e., P_{max}^{PM}) computed from the observed CO_2 flux data increased substantially with increasing NPP (Fig. 3). This P_{max}^{PM} dependence on NPP was found for all biomes examined. P_{max}^{PM} was defined as follows:

$$P_{max}^{PM} = a_{PM}\ \exp\left(b_{PM}\cdot \mathrm{NPP}\right) \quad (6)$$

where a_{PM} (μmol CO_2 m^{-2} s^{-1}) and b_{PM} ((g C m^{-2} y^{-1})$^{-1}$) are constant coefficients empirically determined for each biome by the least-squares method (Table 2).

The initial slope α in Eq. (1) shows the complicated seasonal course of the light response curve and of P_{max}, as shown in previous studies (e.g., Gilmanov et al., 2003). Owen et al. (2007) have shown that α can be expressed as a linear function of canopy CO_2 uptake capacity. Similarly, we found that seasonal variation in α was correlated with that in P_{max} (Fig. 4). Therefore, we defined α as a linear function of P_{max}:

$$\alpha = a_{Ini}\cdot P_{max} + b_{Ini} \quad (7)$$

where a_{Ini} and b_{Ini} are also constant coefficients empirically determined for each biome by the least-squares method (Table 2).

RE is the sum of autotrophic plant respiration and heterotrophic soil respiration, and is usually expressed as a function of soil temperature (e.g., Falge et al., 2001). It has been

Table 2. List of biome-specific parameter values.

Types	Terms	Eq. (3)			Eq. (4)		Eq. (6)		Eq. (7)		Eq. (8)	
		T_{max}	T_{min}	T_{opt}	a_{FV}	b_{FV}	a_{PM}	b_{PM}	a_{Ini}	b_{Ini}	RE_{ref}	Q_{10}
	Units	°C	°C	°C	kPa	–	μmol CO_2 m^{-2} s^{-1}	(g C m^{-2} y^{-1})$^{-1}$	(μmol photon m^{-2} s^{-1})$^{-1}$	μmol CO_2 (μmol photon)$^{-1}$	μmol CO_2 m^{-2} s^{-1}	
ENF		41	1	25	3.78	0.73	14.85	0.0013	0.00075	0.0059	1.48	1.91
EBF		43	2	28	2.14	0.73	11.03	0.0015	0.0014	−0.0058	1.55	2.32
DBF		41	1	25	1.87	0.52	34.64	0.0004	0.00078	0.008	1.88	1.62
MF		40	0	23	3.28	0.60	4.21	0.0045	0.0012	0.0003	1.24	1.61
GRS		40	3	25	1.60	0.56	16.03	0.0013	0.00082	0.0059	1.51	1.94
SVN		40	9	28	1.11	1.55	8.82	0.0043	0.0009	0.0028	0.25	3.36
TND		26	−3	15	0.59	0.60	2.06	0.0108	0.0011	0.0048	0.96	1.49

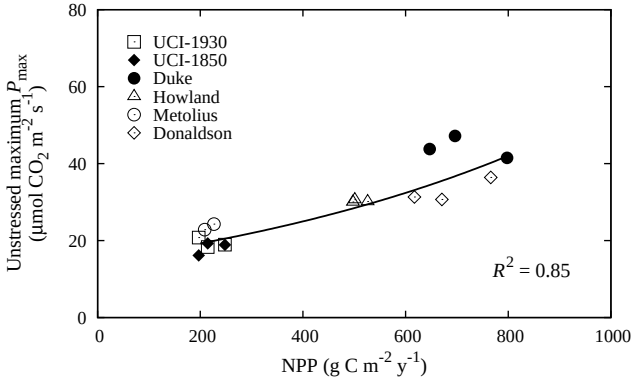

Fig. 3. Relationship between annual NPP and unstressed maximum P_{max} in evergreen needle-leaf forests. Sites are indicated as follows: open squares, UCI-1930 burn; solid diamonds, UCI-1850 burn; solid circles, Duke Forest loblolly pine; open triangles, Howland forest; open circles, Metolius; and open diamonds Slashpine-Donaldson, for each year. The solid line is the regression curve. The square of the correlation coefficient R^2 was determined by the least squares method.

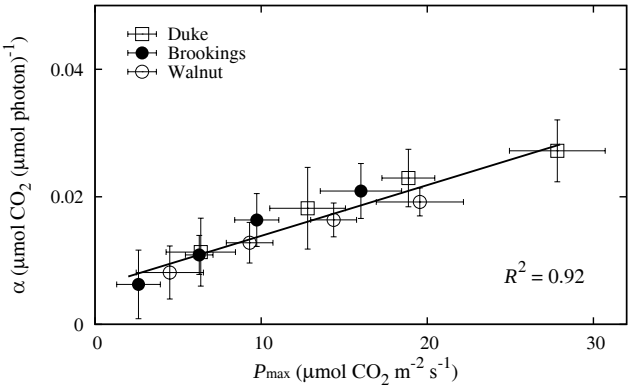

Fig. 4. Relationship between bin-averaged P_{max} and initial slope α in grassland. Sites are indicated as follows: open squares, Duke forest open field; solid circles, Brookings; and open circles, Walnut River Watershed. The solid line is the regression curve, and error bars represent standard deviation from the mean.

further argued that RE varies with differences in short- and long-term temperature sensitivities (Reichstein et al., 2005), the start of the wet season and the timing of rain events (Xu and Baldocchi, 2004), differences in temperature sensitivities among ecosystem sites, even in the same biome (Gilmanov et al., 2007), and photosynthetic rate (Sampson et al., 2007). Accordingly, we can expect that seasonal variation in RE is in part site-specific, so universal attributes are difficult to formulate with a single equation. However, for application over large areas covering numerous biomes, a simple model driven by limited input data is required. We therefore used a traditional exponential relationship between RE and temperature as:

$$RE = RE_{ref}\, Q_{10}^{(T_a-10)/10} \quad (8)$$

where RE_{ref} is the ecosystem respiration rate (μmol CO_2 m^{-2} s^{-1}) when T_a=10°C , and Q_{10} represent the temperature sensitivity of RE. The values of RE_{ref} and Q_{10} were empirically determined for each biome by fitting all available RE data, estimated in the fitting of Eq. (1), to Eq (8) using the least-squares method (Table 2).

To summarize the approach used for modeling diurnal variations in NEE presented in the section above, all parameters required to operate the model involve only four variables: air temperature, VPD, annual precipitation, and PPFD. In applying the model, the parameters P_{max} and α in the nonrectangular hyperbola are estimated by using Eqs. (2) and (7) for each day, whereas the value of P_{max}^{PM} in Eq. (2) is determined for each year using Eq. (6). Hence, diurnal variation in gross primary production (GPP) – the first term on the right-hand side in Eq. (1) – is attributed to changes in the diurnal course of PPFD, as obtained from local observations. On the other hand, RE is estimated for every half-hour or hourly time step, both during the day and at night, with local observed air temperature data in place of T_a in Eq. (8). This assumes that the half-hour or hourly temperature response of RE is the same as that in the 15-day period, the temperature of which was used as the representative mean temperature to determine the

empirical coefficients in Eq. (8). In general, the temperature response of RE is determined using nocturnal eddy covariance CO_2 flux data, and this nocturnal temperature dependence is extrapolated to daytime (e.g., Goulden et al., 1996; Falge et al., 2002). However, nocturnal eddy covariance surface fluxes calculated using typical averaging times of about 30 min generally exhibit large scatter because of measurement error by mesoscale motion, since the cospectral gap, which separates turbulence and mesoscale contributions, is commonly located at a time scale of a few minutes or less during the nocturnal period (e.g., Vickers and Mahrt, 2003). Therefore, we extrapolated the daytime temperature dependence of RE to the night-time dependence (e.g., Suyker and Verma, 2001; Gilmanov et al., 2003).

2.3 Validation data

To examine model validity, we used higher-quality Level 4 products of 10 AmeriFlux ecosystem sites (Table 3). Only the data not used in model construction were selected here. Half-hourly air temperature, VPD, and annual precipitation, used as input data to operate the model, and variability in observed NEE were obtained from Level 4 products, while PPFD data were obtained from quality-checked Level 3 products, since Level 4 does not contain PPFD data.

We also ran the model using the AsiaFlux network data (Fukushima, 2002) to check the simulation performance of the model in regions other than North America. For this check, data from four selected sites, which are located in ENF, EBF, DBF, and MF, were used.

3 Results and discussion

3.1 Variations in parameters among biomes

We examined the relationships between estimated annual NPP and unstressed maximum P_{max} at all sites (Fig. 5a). Increasing NPP was correlated with increasing unstressed maximum P_{max}, regardless of the biome type. Since NPP is estimated using annual mean temperature or annual precipitation, this result suggests that canopy assimilation capacity, to a large degree, depends on temperature and water conditions at the measurement sites. The NPP response of the unstressed maximum P_{max} varied among biomes: the unstressed maximum P_{max} in TND ecosystems was most sensitive to NPP, and that in DBFs was least sensitive (Table 2 and Fig. 5a). The low values of R^2 may be mainly associated with the limited amount of available data, and additional datasets covering various ranges in temperature and precipitation would improve the estimate of unstressed maximum P_{max}.

We plotted regression lines of α, estimated as a linear function of P_{max}, for every biome (Fig. 5b). At the leaf level, previous studies (e.g., Ehleringer and Björkman, 1977; Ehleringer and Pearcy, 1983) have shown that α is nearly universally the same among unstressed plants. At the canopy level in the current analyses, however, α for the seven biomes showed clear seasonal variations; these may result from seasonal changes in the canopy including physiological development and changes in leaf area index (LAI). A remarkable point in Fig. 5b is the similarities in the correlation between P_{max} and α for all biomes analyzed. This result suggests that the relationship between P_{max} and α may be universal, regardless of biome type. A similar result has been reported by Owen et al. (2007). However, little information is available on the physiological mechanisms behind the general relationship between α and P_{max}, and the similarities in the correlation between α and P_{max} may, in part, be the result of poor fitting in Eq. (1). In the following analyses we therefore used the individual regression lines estimated for each biome (see Table 2).

The relationships between temperature and RE for the seven biomes are shown in Fig. 5c. The sensitivities of RE to temperature varied among biomes. SVN had the highest temperature response (Q_{10}=3.36), and the lowest response was found in TND (Q_{10}=1.49) (Table 2). Tjoelker et al. (2001) reported that the Q_{10} value is not constant and declines with increasing temperature for various species, and they represented this fraction in Q_{10} as a function of temperature. In addition, Curiel Yuste et al. (2004) found that the fraction in Q_{10} for soil respiration also depends on seasonal patterns of plant activity, such as changes in LAI. Consideration of this seasonality in Q_{10} may improve RE estimation in the model; however, it would require further investigation of the relationship between the seasonal Q_{10} course and environmental factors. In this study, therefore, simple temperature dependence and constant Q_{10} values estimated for each biome were used to represent the diurnal variations in RE at all ecosystem sites.

Before comparing the observed and predicted diurnal variations in NEE, we compared the seasonal changes in P_{max} (Fig. 6) and α (Fig. 7) computed by the model with the observed changes. Individual points in the graphs are the weekly averaged values of parameters. The seasonal cycle amplitudes of P_{max} and α at the Duke Forest site, an ENF, were larger than those at the other sites. The Santarem site, an EBF, had large values with small amplitudes year round. The results for the DBF and MF sites clearly reflected the existence of both growing and non-growing seasons in a year, while the start and end times of the growing season in the mature red pine site are not shown in the figures because of a lack of data. In contrast, variability of P_{max} and α was always observed at the evergreen sites.

The seasonal courses of the modeled P_{max} and α, and the magnitudes of these two parameters, showed good agreement with observational data from the Duke Forest site. On the other hand, the model did not account for the seasonality in two parameters at the Santarem site. Small variations in temperature and VPD at the site throughout the year resulted in a smooth and small amplitude in parameters estimated by the

Table 3. List of AmeriFlux eddy covariance measurement sites used for validation.

Site	Year	AMT (°C)	AP (mm)
ENF			
UCI-1930 burn site	2005	−1.3	882
Howland forest	2001	7.2	524
Slashpine-Donaldson	2001	19.7	1047
EBF			
Florida-Kennedy Space Center	2002	21.2	932
DBF			
Harvard Forest EMS Tower	2004	7.6	1175
Missouri Ozark Site	2007	13.7	645
MF			
Mature red pine	2002	6.4	640
GRS			
Brookings	2004	7.6	831
SVN			
Audubon Research Ranch	2003	16.5	353
TND			
Barrow	1999	−11.3	94

model. However, the model captured mean magnitudes of parameters when compared with observed values. For DBF and MF sites, the model captured the seasonality of P_{max} and α, and the approximate timing of the start and end of ecosystem productivity, but overestimates of P_{max} were found at the Bartlett site. This overestimation of P_{max} during the growing season is due to the overestimated P_{max}^{PM} in Eq. (2), which was estimated from the annual NPP computed using the Miami model. Additional data from new sites may lead to an alteration of the constant coefficients empirically determined for individual parameters.

3.2 Variations in NEE

Next, to demonstrate the capability of the proposed model, we ran the model for 10 AmeriFlux ecosystem sites with data for a year not used in the model development (Table 3). Variations in half-hourly NEE were calculated for all sites during the entire period for which input meteorological data were available (Fig. 8). At the Slashpine-Donaldson site, in an ENF, net CO_2 uptake was observed during daytime year round, but at the Howland site in an ENF, NEE was very close to 0 μmol CO_2 m^{-2} s^{-1} during the period between the end of the year and spring. The model successfully predicted these seasonal variations in NEE; in addition, it predicted the diurnal variations, such as when NEE becomes positive or negative, for both ENF and EBF sites.

On the other hand, the model underestimated the length of the net CO_2 uptake periods at the Missouri Ozark and Brookings sites (DBF and GRS, respectively), and did not predict

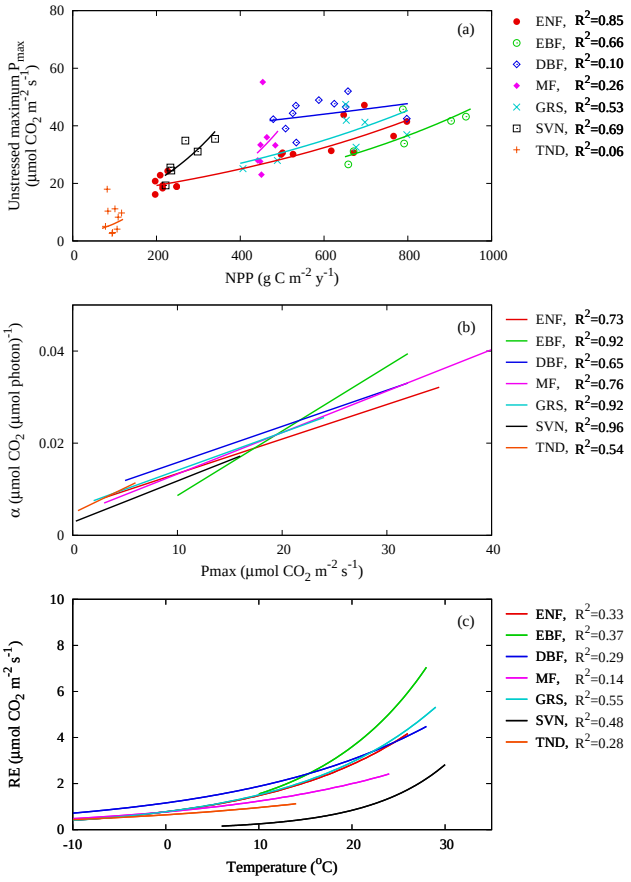

Fig. 5. Distributions of three parameters for seven biomes. **(a)** Same as Fig. 3, but for all biomes analyzed, **(b)** relationships between P_{max} and α, and **(c)** between temperature and RE. Red: evergreen needle-leaf forests (ENF); green: evergreen broadleaf forests (EBF); blue: deciduous broadleaf forests (DBF); magenta: mixed forests (MF); lightblue: grasslands (GRS); black: savanna (SVN); and orange: tundra (TND).

the low observed negative NEE during the daytime in winter (Fig. 8). This is because net CO_2 uptake was observed at both sites, even in winter when T_a <0°C, while the minimum temperatures for photosynthesis in this model were set to 1°C for DBF and 3°C for GRS (Table 2). Burba et al. (2008) reported that CO_2 flux measured with an open-path gas analyzer can yield unreasonable CO_2 uptake values under low-temperature conditions, due to heating of the instrument body. Differences in NEE between the observations and the model during the winter may result partly from this problem.

Overall, the predicted diurnal and seasonal patterns of CO_2 uptake and release agree with the observed data, except for the SVN at the Audubon Research Ranch and the TND at the Barrow site. For SVN and TND, the model failed in the prediction of NEE variations, especially for SVN. The errors for these two biomes will be revisited later in this section. The degree of model prediction for half-hourly variations in the observed NEE was evaluated by regression analysis. At individual sites, the values of R^2, slope, and y-intercept

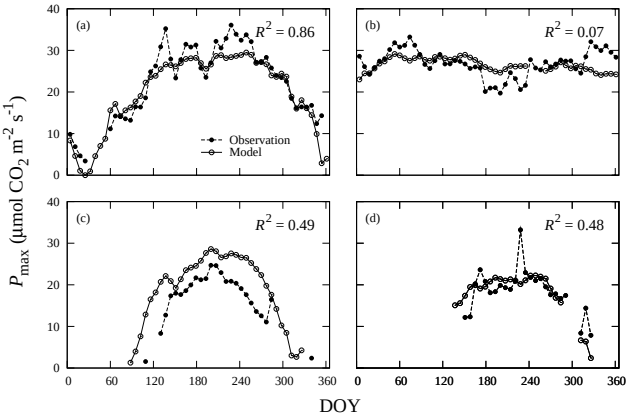

Fig. 6. Seasonal course of weekly averaged P_{max} at **(a)** the Duke Forest site, ENF, in 2004; **(b)** the Santarem site, EBF, in 2003; **(c)** the Bartlett site, DBF, in 2004; and **(d)** the mature red pine site, MF, in 2004. The dashed line with closed circles represents P_{max} estimated from the observed data, and the solid line with open circles is P_{max} predicted using the proposed model. DOY=day of year.

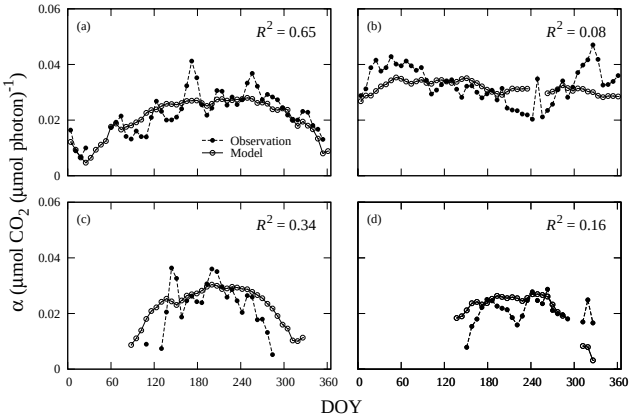

Fig. 7. Same as Fig. 6, but for α.

were between 0.55 and 0.84, 0.59 and 0.90, and −2.07 and 0.74, respectively (Table 4), when all available half-hourly NEE data were used. The model explained only 55% of the half-hourly variations in NEE at the Missouri Ozark site (N=17 468), but explained 84% of the NEE variations in the UCI-1930 burn site (N=3259). These results suggest that differences exist between predicted and observed NEE, and that the degree of agreement is site-dependent. However, the observation records often contain noise that, to some extent, is due to measurement error. To reduce the influence of measurement error and smooth the variability in NEE, the observed and predicted NEE data were averaged for each half-hourly interval over 10-day periods.

The model performance improved considerably when the 10-day averaged half-hourly NEE variations were used (Table 4 and Fig. 9). At six forest sites, except the Missouri Ozark and Brookings sites, the model provided acceptable values of R^2, ranging between 0.83 and 0.95. The slope of the regression line was 0.63 at the Howland forest site, but this small slope value is partly attributable to model underestimation of RE at night. Indeed, the slope of the regression line was improved to 0.72 at the Howland forest site when only daytime NEE data were used. Nighttime RE will be discussed in the next subsection.

In contrast to the six forest sites described above, the model explained only 65% of 10-day averaged half-hourly NEE variations at the Missouri Ozark site. A steep net uptake of CO_2 was observed at this site after DOY 120 in 2007, and this net uptake rapidly decreased around DOY 220 (Fig. 8). However, the model predicted smooth net uptake over the period between DOY 60 and 330, which resulted in large differences between observed and predicted NEE, as shown in Fig. 9. The rapid changes in amplitude of diurnal NEE variations during the growing season may be mainly associated with the rapid changes in LAI. Moderate Resolution Imaging Spectroradiometer (MODIS) MOD15A2 products indicated that LAI increased from 0.9 on DOY 121 in 2007 to 3.7 on DOY 129, and decreased from 4.2 on DOY 209 to 2.2 on DOY 225, and these drastic variation in LAI seem to be consistent with those in NEE.

The low value of R^2 at the Brookings site (R^2=0.65) is attributed, in part, to the low CO_2 uptake observed from DOY 200 to DOY 260 (Fig. 8). A daytime maximum NEE of $-11.3\,\mu$mol CO_2 m^{-2} s^{-1} was observed for DOY 171–180, but daytime NEE decreased to $-3.2\,\mu$mol CO_2 m^{-2} s^{-1} for DOY 221–230, and increased again to $-7.6\,\mu$mol CO_2 m^{-2} s^{-1} for DOY 261–270. One possible explanation for the low negative NEE observed in this period is disturbance such as grazing and mowing. Grazing intensity markedly affects aboveground biomass (e.g., Cao et al., 2004) and can thus cause variations in ecosystem productivity. However, the MOD15A2 products did not show drastic changes in LAI during the period from DOY 200 to 260; thus, this pattern remains to be explained.

Daytime NEE observed at the Audubon and Barrow sites varied during the growing season (Fig. 8). High CO_2 release was observed at both sites during the daytime around DOY 180, but NEE changed to net CO_2 uptake a few weeks later. At the Audubon site, analysis of the observation data revealed that the duration of the assimilation period was narrowly restricted to about 100 days, and the seasonal patterns of the physiological parameters were very sharp. These processes were less sensitive to changes in temperature and VPD than in other biomes. Leuning et al. (2005) have shown that the productivity of a SVN ecosystem is controlled almost exclusively by the amount and timing of rainfall during the wet season. Ma et al. (2007) similarly noted that both photosynthesis and respiration processes in SVN depend on the amount of seasonal precipitation. These previous studies suggest that precipitation is the dominant factor controlling SVN ecosystem productivity under drought

Table 4. Slopes (a), intercepts (b), and R^2 values of regression lines, y=ax+b, between the observed and modeled NEE, and the number of observations (N) at 10 AmeriFlux sites. The y-axis values are model predictions and the x-axis values are the observations. $_{all}$ represents the values calculated from all available half-hourly NEE data, and $_{10\,day}$ the values from NEE averaged at half-hourly intervals over 10-day periods.

Site	a_{all}	$a_{10\,day}$	b_{all}	$b_{10\,day}$	R^2_{all}	$R^2_{10\,day}$	N_{all}	$N_{10\,day}$
UCI-1930 burn site, ENF	0.79	0.84	−0.25	−0.19	0.84	0.95	3259	390
Howland forest, ENF	0.59	0.63	−0.66	−0.64	0.79	0.90	17 518	1728
Slashpine-Donaldson, ENF	0.85	1.00	−2.07	−1.85	0.69	0.83	17 424	1728
Florida-Kennedy Space Center, EBF	0.71	0.74	0.74	0.75	0.82	0.91	13 408	1392
Harvard Forest EMS Tower, DBF	0.79	0.81	−1.52	−1.44	0.83	0.89	12 338	1294
Missouri Ozark Site, DBF	0.90	1.04	−1.64	−1.53	0.55	0.65	17 468	1728
Mature red pine, MF	0.82	0.94	−1.37	−0.43	0.72	0.84	7890	864
Brookings, GRS	0.68	0.73	−1.04	−1.02	0.59	0.65	12 114	1221
Audubon Research Ranch, SVN	−0.21	−0.29	−0.75	−0.68	0.03	0.05	17 376	1728
Barrow, TND	0.10	0.15	−0.32	−0.25	0.13	0.23	4362	480

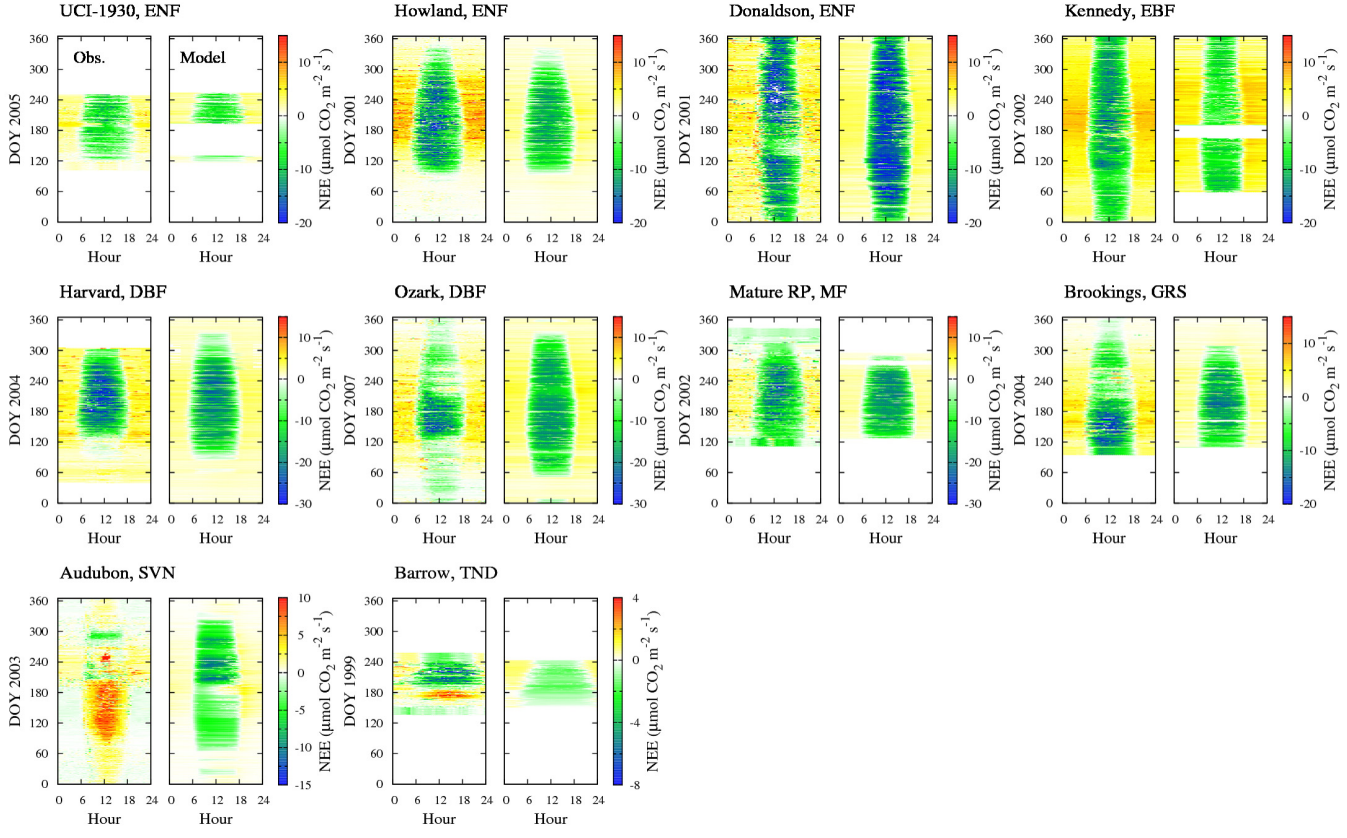

Fig. 8. Diurnal and seasonal patterns of observed (left) and predicted (right) NEE at 10 AmeriFlux ecosystem sites. The magnitudes of half-hourly NEE are represented by colors. The blank spaces in the figure, such as the period between DOY 1 and about DOY 100 for the UCI-1930 site, are due to gaps in NEE and meteorological data.

conditions. Figure 10 shows the seasonal courses of LAI from the MOD15A2 products and daily precipitation at the Audubon site in 2003. LAI was nearly constant, ranging from 0.2 to 0.3, during the dry period before DOY 190, but rapidly increased following the rainfall events that occurred frequently after DOY 192. An LAI of 0.3 on DOY 193 increased to 0.8 on DOY 209. Figures 8 and 10 clearly show that plant development and CO_2 gas exchange at the

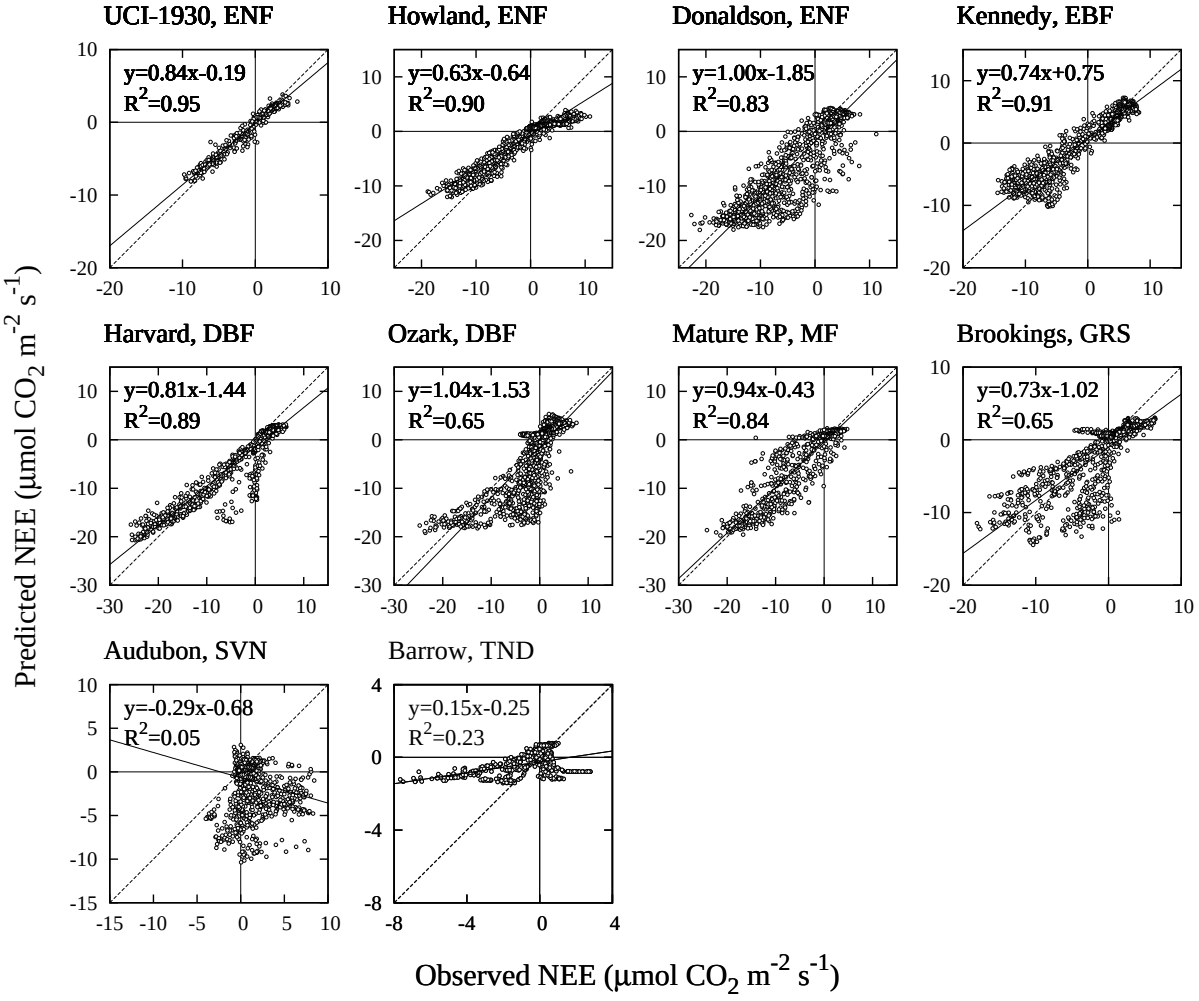

Fig. 9. Comparisons between half-hourly variations in observed and predicted NEE, averaged over 10-day periods, at 10 AmeriFlux ecosystem sites. The open circles represent NEE, solid lines are regression lines, and dashed lines are y=x.

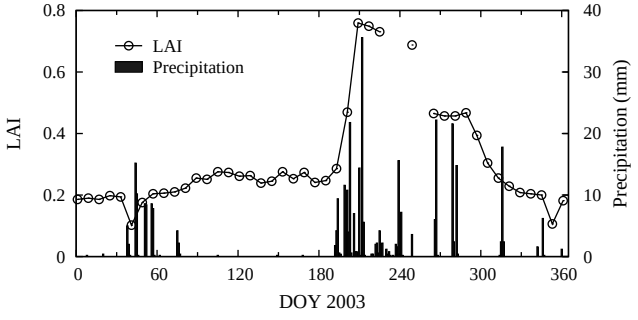

Fig. 10. Seasonal courses of LAI, from the MOD15A2 for the areas surrounding the Audubon Research Ranch site, and daily precipitation in 2003. Open circles represent LAI and bars precipitation.

Audubon SVN site are mainly limited by water stress, as discussed by Leuning et al. (2005) and Ma et al. (2007).

For the Barrow site, LAI data for 1999 were not available from the MOD15A2 products, and the relationship between LAI and rapid changes in NEE could not be examined. However, Harazono et al. (2003) reported that photosynthetic activity on the flooded Barrow TND is immediately observed after snowmelt, which strongly influences the rapid development of TND vegetation. Although further investigation using local observation data is required, drastic changes in NEE at the Barrow site, shown in Fig. 8, could be explained by the seasonal course of LAI at the site.

Despite the simplicity of the proposed model and its basis in empirical regression methods driven by four environmental parameters, it performed well for half-hourly variations in NEE over long periods, particularly for forest biomes. These results indicate that the nonrectangular hyperbola with biome-specific seasonality of physiological parameters can be applied to various biomes to predict diurnal variations in NEE. However, at some of the sites with very rapid changes in LAI, there was poor agreement between observed

and predicted NEE. Because the proposed model does not use any plant physiological information to estimate diurnal variations in NEE, the model cannot predict rapid changes in NEE associated with changes in LAI. Yuan et al. (2007) developed a light-use-efficiency model using information from a normalized difference vegetation index (NDVI) that was able to predict seasonal variability in GPP in GRS and SVN biomes. Similarly, Leuning et al. (2005) estimated seasonal variability in a SVN during the wet season using MODIS data. These remote-sensing data products respond directly to changes in overall canopy conditions such as LAI and canopy structure. For future studies, these data may be useful for further improvement of the proposed model.

3.3 Nocturnal RE

As mentioned above, the model uses the response of daytime ecosystem respiration to temperature to estimate variability between daytime and nighttime RE over the entire period. To demonstrate the ability of the model to predict RE variability, we show the observed and modeled seasonal course of monthly averaged nocturnal RE at the Howland and Donaldson sites (ENF) and the Missouri Ozark site (DBF), for which nocturnal RE data are available over the entire period (Fig. 11). The model captures the seasonal cycle of nocturnal RE at the Donaldson and Missouri Ozark sites, but the computed amplitudes are somewhat smaller than those of the observation data. For these two sites, the model slightly underestimates RE in summer; the difference between the observations and the model is approximately 1.7 μmol CO_2 m^{-2} s^{-1}. This discrepancy could be attributed to the simplifying approach of the model. In the interest of constructing the model as simply as possible, RE variability over a year was introduced using a single equation as a function of temperature for each biome, regardless of differences in soil conditions and plant developmental stages. Sampson et al. (2007), for example, demonstrated that there is considerable variability in the temperature dependence of soil respiration associated with seasonal differences in photosynthesis. However, to avoid complexity and obviate the need to obtain additional information on the mechanics of the relationship between RE and photosynthesis, the model does not account for the influence of these physiological activities on RE. On the other hand, as shown by the large error bars in Fig. 11, it is also clear that the nocturnal eddy covariance data provide large scatter associated with weak turbulence. This noise is mainly due to flux sampling errors, which may, in part, be the cause of the difference between the observed and predicted RE.

In contrast to the Donaldson and Missouri Ozark sites, modeled nocturnal RE was clearly much lower than observed nocturnal RE at the Howland site during the growing season. The model predicted an average nocturnal RE of 2.2 μmol CO_2 m^{-2} s^{-1} in July, while the observed data were 7.8 μmol CO_2 m^{-2} s^{-1}. Air temperature at the Howland site was generally lower than that at the Donaldson site

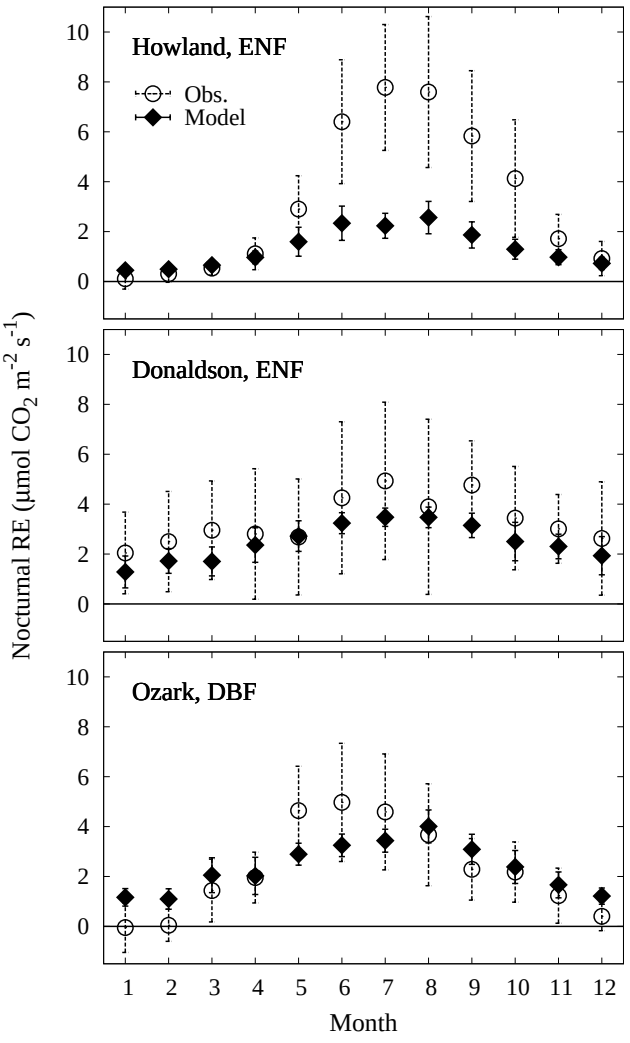

Fig. 11. Seasonal course of monthly averaged nocturnal RE at the Howland ENF site in 2001, the Donaldson ENF site in 2001, and the Ozark DBF site in 2007. A dashed line with open circles represents observed data, and a solid line with closed diamonds is the model data. Error bars represent the standard deviation from the mean.

year round, which resulted in the lower predicted RE at the Howland site, since the proposed model estimates RE using the same temperature response for the same biome. However, higher nocturnal RE observed at the Howland site during the growing season compared to that at the Donaldson site led to the model being unable to predict this site-specific variability in RE. This high observed nocturnal RE at the Howland site may, in part, be due to carbon richness of the soil, although no detailed evidence exists to support this proposal. It is important to be aware of the abovementioned problems when computing RE variability using the model.

3.4 Application to AsiaFlux ecosystems

To validate the applicability of the proposed empirical model, constructed with the AmeriFlux data sets, to other regions,

Table 5. Same as Table 1, but for AsiaFlux eddy covariance measurement sites analyzed.

Site, country	Year	Latitude, longitude	AMT (°C)	AP (mm)	Reference
ENF					
Fujiyoshida forest meteorology research site, Japan	2000	34.45° N, 138.76° E	9.6	1599	Ohtani et al. (2005)
EBF					
Sakaerat, Thailand	2002	14.29° N, 101.55° E	24.4	1813	Gamo and Panuthai (2005)
DBF					
Mae Klong, Thailand	2003	14.34° N, 98.50° E	24.7	1708	Huete et al. (2008)
MF					
CC-LaG experiment site, Japan	2002	45.03° N, 142.06° E	5.6	973	Takagi et al. (2005)

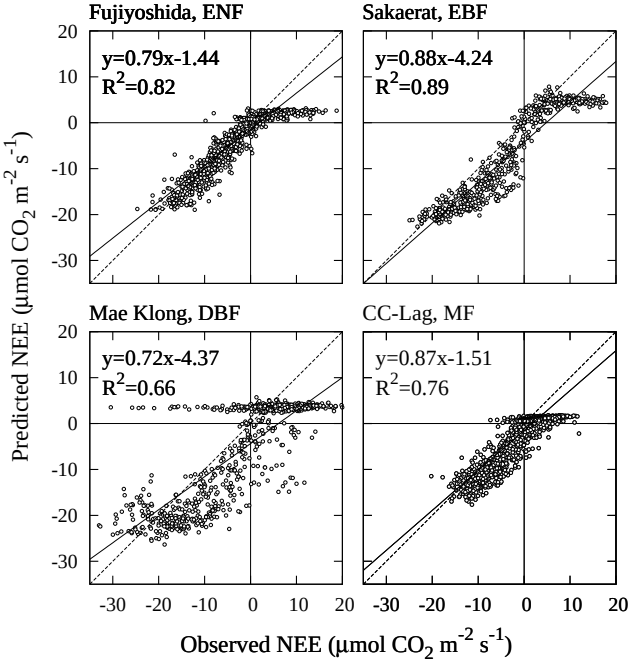

Fig. 12. Same as Fig. 9, but for four AsiaFlux ecosystem sites.

we applied the model to data obtained from the AsiaFlux network. Details of individual ecosystem sites can be found in Table 5. All half-hourly or hourly CO_2 fluxes were measured at four forest sites using the eddy covariance method. Micrometeorological data such as air temperature and PPFD were also obtained from the AsiaFlux network. The ecosystem-specific parameter values, such as T_{max} in Eq. (3) and a_{FV} in Eq. (4), from the AmeriFlux network listed in Table 2 were used without any modifications to estimate variations in half-hourly or hourly NEE in the AsiaFlux forest sites.

Figure 12 shows comparisons between the observations and model results of 10-day averaged half-hourly or hourly NEE variations at each site, as in Fig. 9. Overall, the model gave reasonable predictions of NEE variation during the daytime CO_2 uptake period, although scatter was rather large at the Mae Klong DBF site. The values of R^2 at three sites, apart from the Mae Klong site, ranged from 0.76 to 0.89, which are comparable to the results obtained using the model on the AmeriFlux sites. This result suggests that the environmental forces used in this model are critical determinants of photosynthesis in various biomes, and that the biome-specific responses to environmental forces, determined by the AmeriFlux data, may be applicable to other regions. However, it is evident that there was a discrepancy between observed and predicted nocturnal RE, and that the model produced systematic underestimates. Unfortunately, this study was unable to generalize the variation in RE in response to temperature; therefore, accurate modeling of RE is necessary to substantially improve the model's simulation of long-term diurnal CO_2 exchange.

4 Conclusions

We explored a simple approach to predicting diurnal variations in NEE over seven biomes and proposed an empirical model based on the use of a nonrectangular hyperbola and eddy covariance flux data obtained from the AmeriFlux network. Physiological parameters in the nonrectangular hyperbola – P_{max}, α and RE – clearly exhibited seasonal variations. While these seasonal variations were complex, P_{max} and α generally showed a dependence on temperature and VPD, and the degree of this dependence varied among biomes. The study expressed the seasonality in parameters as a function of only environmental variables – air temperature, VPD, and precipitation – for each biome, and diurnal variability in NEE was predicted using these biome-specific parameters together with PPFD. The proposed model successfully predicted the diurnal variability of NEE for almost all forest biomes in the AmeriFlux network over the entire annual observation period. However, the model was unable to account for drastic changes in the magnitude of NEE and CO_2 uptake and release associated with rapid changes in LAI that were mainly observed in SVN and TND ecosystems. The model demonstrated acceptable performance for

the AsiaFlux ecosystem sites, although further refinement is needed for RE. Therefore, the approach used in this study should be applicable to many other regions. Adjustment of the methodology used in parameter estimations, application of remote-sensing products, and subdivision of the biome types would further improve the precision of the model.

Acknowledgements. This study is conducted at the GOSAT project at NIES, Japan. We thank Yanhong Tang at NIES for useful comments on the manuscript, and the AmeriFlux and AsiaFlux networks and the NOAA Earth System Research Laboratory and Pennsylvania State University for providing the data. Data for the Bartlett and Howland sites were provided by the Northeastern States Research Cooperative, under support by the US Department of Energy (DOE) through the Office of Biological and Environmental Research (BER) Terrestrial Carbon Processes (TCP) program (No. DE-AI02-07ER64355) with additional support from the USDA Forest Services Northern Global Change program and Northern Research Station, and those for the Duke sites were supported by the DOE through the BER TCP program (No. 10509-0152, DE-FG02-00ER53015, and DE-FG02-95ER62083).

Edited by: G. Wohlfahrt

References

Baldocchi, D. D.: "Breathing" of the terrestrial biosphere: lessons learned from a global network of carbon dioxide flux measurement systems, Aust. J. Bot., 56, 1–26, 2008.

Bonan, G. B.: A land surface model (LSM version 1.0) for ecological, hydrological, and atmospheric studies: Technical description and user's guide, NCAR Tech. Note NCAR/TN-417+STR, 1996.

Bonan, G. B.: The land surface climatology of the NCAR Land Surface Model coupled to the NCAR Community Climate Model, J. Climate, 11, 1307–1326, 1998.

Burba, G. G., McDermitt, D. K., Grelle, A., Anderson, D. J., and Xu, L.: Addressing the influence of instrument surface heat exchange on the measurements of CO_2 flux from open-path gas analyzers, Glob. Change Biol., 14, 1854–1876, 2008.

Cao, G., Tang, Y., Mo, W., Wang, Y., Li, Y., and Zhao, X.: Grazing intensity alters soil respiration in an alpine meadow on the Tibetan plateau, Soil Biol. Biochem., 36, 237–243, 2004.

Curiel Yuste, J., Janssens, I. A., Carrara, A., and Ceulemans, R.: Annual Q_{10} of soil respiration reflects plant phenological patterns as well as temperature sensitivity, Glob. Change Biol., 10, 161–169, 2004.

Dore, S., Hymus, G. J., Johnson, D. P., Hinkle, C. R., Valentini, R., and Drake, B. G.: Cross validation of open-top chamber and eddy covariance measurements of ecosystem CO_2 exchange in a Florida scrub-oak ecosystem, Glob. Change Biol., 9, 84–95, 2003.

Ehleringer, J. and Björkman, O.: Quantum yield for CO_2 uptake in C_3 and C_4 plants, Plant Physiol., 59, 86–90, 1977.

Ehleringer, J. and Pearcy, R. W.: Variation in quantum yield for CO_2 uptake among C_3 and C_4 plants, Plant Physiol., 73, 555–559, 1983.

Epstein, H. E., Calef, M. P., Walker, M. D., Chapin, F. S., and Starfield, A. M.: Detecting changes in arctic tundra plant communities in response to warming over decadal time scales, Glob. Change Biol., 10, 1325–1334, 2004.

Eugster, W., Rouse, W. R., Pielke, R. A., McFadden, J. P., Baldocchi, D. D., Kittel, T. G. F., Chapin, F. S., Liston, G. E., Vidale, P. L., Vaganov, E., and Chambers, S.: Land-atmosphere energy exchange in Arctic tundra and boreal forest: available data and feedbacks to climate, Glob. Change Biol., 6, 84–115, 2000.

Falge, E., Baldocchi, D., Olson, R., Anthoni, P., Aubinet, M., Bernhofer, C., Burba, G., Ceulemans, R., Clement, R., Dolman, H., Granier, A., Gross, P., Grünwald, T., Hollinger, D., Jensen, N. O., Katul, G., Keronen, P., Kowalski, A., Lai, C. T., Law, B. E., Meyers, T., Moncrieff, J., Moors, E., Munger, J. W., Pilegaard, K., Rannik, Ü., Rebmann, C., Suyker, A., Tenhunen, J., Tu, K., Verma, S., Vesala, T., Wilson, K., and Wofsy, S.: Gap filling strategies for defensible annual sums of net ecosystem exchange, Agric. Forest Meteorol., 107, 43–69, 2001.

Falge, E., Baldocchi, D., Tenhunen, J., Aubinet, M., Bakwin, P., Berbigier, P., Bernhofer, C., Burba, G., Clement, R., Davis, K. J., Elbers, J. A., Goldstein, A. H., Grelle, A., Granier, A., Guðmundsson, J., Hollinger, D., Kowalski, A. S., Katul, G., Law, B. E., Malhi, Y., Meyers, T., Monson, R. K., Munger, J. W., Oechel, W., Paw U, K. T., Pilegaard, K., Rannik, Ü., Rebmann, C., Suyker, A., Valentini, R., Wilson, K., and Wofsy, S.: Seasonality of ecosystem respiration and gross primary production as derived from FLUXNET measurements, Agric. Forest Meteorol., 113, 53–74, 2002.

Farquhar, G. D., von Caemmerer, S., and Berry, J. A.: A biochemical model of photosynthetic CO_2 assimilation in leaves of C_3 species, Planta, 149, 78–90, 1980.

Fukushima, Y.: Perspective of AsiaFlux, AsiaFlux Newsletter, 2, 1–2, 2002.

Fung, I. Y., Tucker, C. J., and Prentice, K. C.: Application of Advanced Very High Resolution Radiometer vegetation index to study atmosphere-biosphere exchange of CO_2, J. Geophys. Res., 92, 2999–3015, 1987.

Gamo, M. and Panuthai, S.: Carbon flux observation in the tropical seasonal evergreen forest in Sakaerat, Thailand, AsiaFlux Newsletter, 14, 4–6, 2005.

Gholz, H. L. and Clark, K. L.: Energy exchange across a chronosequence of slash pine forests in Florida, Agric. Forest Meteorol., 112, 87–102, 2002.

Gilmanov, T. G., Verma, S. B., Sims, P. L., Meyers, T. P., Bradford, J. A., Burba, G. G., and Suyker, A. E.: Gross primary production and light response parameters of four Southern Plains ecosystems estimated using long-term CO_2-flux tower measurements, Global Biogeochem. Cy., 17, 1071, doi:10.1029/2002GB002023, 2003.

Gilmanov, T. G., Tieszen, L. L., Wylie, B. K., Flanagan, L. B., Frank, A. B., Haferkamp, M. R., Meyers, T. P., and Morgan, J. A.: Integration of CO_2 flux and remotely-sensed data for primary production and ecosystem respiration analyses in the Northern Great Plains: potential for quantitative spatial extrapolation, Global Ecol. Biogeogr, 14, 271–292, 2005.

Gilmanov, T. G., Soussana, J. F., Aires, L., Ammann, C., Balzarola, M., Barcza, Z., Bernhofer, C., Campbell, C. L., Cernusca, A., Cescatti, A., Clifton-Brown, J., Dirks, B. O. M., Dore, S., Eugster, W., Fuhrer, J., Gimeno, C., Gruenwald, T., Haszpra, L., Hensen, A., Ibrom, A., Jacobs, A. F. G., Jones, M. B., Lanigan, G., Laurila, T., Lohila, A., Manca, G., Marcolla, B., Nagy,

Z., Pilegaard, K., Pinter, K., Pio, C., Raschi, A., Rogiers, N., Sanz, M. J., Stefani, P., Sutton, M., Tuba, Z., Valentini, R., and Williams, M. L.: Partitioning European grassland net ecosystem CO_2 exchange into gross primary productivity and ecosystem respiration using light response function analysis, Agr. Ecosyst. Environ., 121, 93–120, 2007.

Goulden, M. L., Munger, J. W., Fan, S. M., Daube, B. C., and Wofsy, S. C.: Measurements of carbon sequestration by long-term eddy covariance: methods and a critical evaluation of accuracy, Glob. Change Biol., 2, 169–182, 1996.

Gu, L., Meyers, T., Pallardy, S. G., Hanson, P. J., Yang, B., Heuer, M., Hosman, K. P., Riggs, J. S., Sluss, D., and Wullschleger, S. D.: Direct and indirect effects of atmospheric conditions and soil moisture on surface energy partitioning revealed by a prolonged drought at a temperate forest site, J. Geophys. Res., 111, D16102, doi:10.1029/2006JD007161, 2006.

Harazono, Y., Mano, M., Miyata, A., Zulueta, R. C., and Oechel, W. C.: Inter-annual carbon dioxide uptake of a wet sedge tundra ecosystem in the Arctic, Tellus B, 55, 215–231, 2003.

Hargrove, W. W., Hoffman, F. M., and Law, B. E.: New analysis reveals representativeness of AmeriFlux network, Eos Trans. AGU, 84(48), 529 pp., 2003.

Hirata, R., Saigusa, N., Yamamoto, S., Ohtani, Y., Ide, R., Asanuma, J., Gamo, M., Hirano, T., Kondo, H., Kosugi, Y., Li, S., Nakai, Y., Takagi, K., Tani, M., and Wang, H.: Spatial distribution of carbon balance in forest ecosystems across East Asia, Agric. Forest Meteorol., 148, 761–775, 2008.

Hollinger, D. Y., Aber, J., Dail, B., Davidson, E. A., Goltz, S. M., Hughes, H., Leclerc, M., Lee, J. T., Richrdson, A. D., Rodrigues, C., Scott, N. A., Varier, D., and Walsh, J.: Spatial and temporal variability in forest-atmospheric CO_2 exchange, Glob. Change Biol., 10, 1689–1706, 2004.

Huete, A. R., Restrepo-Coupe, N., Ratana, P., Didan, K., Saleska, S. R., Ichii, K., Panuthai, S., and Gamo, M.: Multiple site tower flux and remote sensing comparisons of tropical forest dynamics in Monsoon Asia, Agric. Forest Meteorol., 148, 748–760, 2008.

Jenkins, J. P., Richardson, A. D., Braswell, B. H., Ollinger, S. V., Hollinger, D. Y., and Smith, M. L.: Refining light-use efficiency calculations for a deciduous forest canopy using simultaneous tower-based carbon flux and radiometric measurements, Agric. Forest Meteorol., 143, 64–79, 2007.

Johnson, I. R. and Thornley, J. H. M.: A model of instantaneous and daily canopy photosynthesis, J. Theor. Biol., 107, 531–545, 1984.

Katul, G., Leuning, R., and Oren, R.: Relationship between plant hydraulic and biochemical properties derived from a steady-state coupled water and carbon transport model, Plant Cell Environ., 26, 339–350, 2003.

Katul, G. G., Hsieh, C., Bowling, D., Clark, K., Shurpali, N., Turnipseed, A., Albertson, J., Tu, K., Hollinger, D., Evans, B., Offerle, B., Anderson, D., Ellsworth, D., Vogel, C., and Oren, R.: Spatial variability of turbulent fluxes in the roughness sublayer of an even-aged pine forest, Bound.-Lay. Meteorol., 93, 1–28, 1999.

Kosugi, Y., Tanaka, H., Takanashi, S., Matsuno, N., Ohta, N., Shibata, S., and Tani, M.: Three years of carbon and energy fluxes from Japanese evergreen broad-leaved forest, Agric. Forest Meteorol., 132, 329–343, 2005.

LeMone, M. A., Grossman, R. L., McMillen, R. T., Liou, K. N., Ou, S. C., McKeen, S., Angevine, W., Ikeda, K., and Chen, F.: Cases-97: Late-morning warming and moistening of the convective boundary layer over the Walnut River Watershed, Bound.-Lay. Meteorol., 104, 1–52, 2002.

Leuning, R., Cleugh, H. A., Zegelin, S. J., and Hughes, D.: Carbon and water fluxes over a temperate *Eucalyptus* forest and a tropical wet/dry savanna in Australia: measurements and comparison with MODIS remote sensing estimates, Agric. Forest Meteorol., 129, 151–173, 2005.

Lieth, H.: Modeling the primary productivity of the world, in: Primary Productivity of the Biosphere, edited by: Lieth, H. and Whittaker, R. H., Springer-Verlag, 237–263, 1975.

Ma, S., Baldocchi, D. D., Xu, L., and Hehn, T.: Inter-annual variability in carbon dioxide exchange of an oak/grass savanna and open grassland in California, Agric. Forest Meteorol., 147, 157–171, 2007.

Martens, C. S., Shay, T. J., Mendlovitz, H. P., Matross, D. M., Saleska, S. R., Wofsy, S. C., Woodward, W. S., Menton, M. C., De Moura, J. M. S., Crill, P. M., De Moraes, O. L. L., and Lima, R. L.: Radon fluxes in tropical forest ecosystems of Brazilian Amazonia: night-time CO_2 net ecosystem exchange derived from radon and eddy covariance methods, Glob. Change Biol., 10, 618–629, 2004.

McMillan, A. M. S., Winston, G. C., and Goulden, M. L.: Age-dependent response of boreal forest to temperature and rainfall variability, Glob. Change Biol., 14, 1904–1916, 2008.

Monteith, J. L.: Solar radiation and productivity in tropical ecosystems, J. Appl. Ecol., 9, 747–766, 1972.

Nemry, B., Francois, L., Gérard, J. C., Bondeau, A., Heimann, M., and the participants of the Potsdam NPP Model Intercomparison: Comparing global models of terrestrial net primary productivity (NPP): analysis of the seasonal atmospheric CO_2 signal, Glob. Change Biol., 5, 65–76, 1999.

Ohtani, Y., Mizoguchi, Y., Watanabe, T., and Yasuda, Y.: Parameterization of NEP for gap-filling in a cool-temperate coniferous forest in Fujiyoshida, Japan, Journal of Agricultural Meteorology, 60(5), 769–772, 2005.

Owen, K. E., Tenhunen, J., Reichstein, M., Wang, Q., Falge, E., Geyer, R., Xiao, X., Stoy, P., Ammann, C., Arain, A., Aubinet, M., Bernhofer, C., Chojnicki, B. H., Granier, A., Gruenwald, T., Hadley, J., Heinesch, B., Hollinger, D., Knohl, A., Kutsch, W., Lohila, A., Meyers, T., Moors, E., Moureau, C., Pilegaard, K., Saigusa, N., Verma, S., Vesala, T., and Vogel, C.: Linking flux network measurements to continental scale simulations: ecosystem carbon dioxide exchange capacity under non-water-stressed conditions, Glob. Change Biol., 13, 734–760, 2007.

Peat, W. E.: Relationships between photosynthesis and light intensity in the tomato, Ann. Bot.-London, 34, 319–328, 1970.

Potter, C. S., Randerson, J. T., Field, C. B., Matson, P. A., Vitousek, P. M., Moonet, H. A., and Klooster, S. A.: Terrestrial ecosystem production: a process model based on global satellite and surface data, Global Biogeochem. Cy., 7, 811–841, 1993.

Rabinowitch, E. I.: Photosynthesis and Related Processes, Interscience Publishers, 1951.

Randerson, J. T., Thompson, M. V., Conway, T. J., Fung, I. Y., and Field, C. B.: The contribution of terrestrial sources and sinks to trends in the seasonal cycle of atmospheric carbon dioxide, Global Biogeochem. Cy., 11, 535–560, 1997.

Reichstein, M., Falge, E., Baldocchi, D., Papale, D., Aubinet,

M., Berbigier, P., Bernhofer, C., Buchmann, N., Gilmanov, T., Granier, A., Grünwald, T., Havránková, K., Ilvesniemi, H., Janous, D., Knohl, A., Laurila, T., Lohila, A., Loustau, D., Matteucci, G., Meyers, T., Miglietta, F., Ourcival, J. M., Pumpanen, J., Rambal, S., Rotenberg, E., Sanz, M., Tenhunen, J., Seufert, G., Vaccari, F., Vesala, T., Yakir, D., and Valentini, R.: On the separation of net ecosystem exchange into assimilation and ecosystem respiration: review and improved algorithm, Glob. Change Biol., 11, 1424–1439, 2005.

Ruimy, A., Dedieu, G., and Saugier, B.: TURC: a diagnostic model of continental gross primary productivity and net primary productivity, Global Biogeochem. Cy., 10, 269–285, 1996.

Saigusa, N., Yamamoto, S., Hirata, R., Ohtani, Y., Ide, R., Asanuma, J., Gamo, M., Hirano, T., Kondo, H., Kosugi, Y., Li, S., Nakai, Y., Takagi, K., Tani, M., and Wang, H.: Temporal and spatial variations in the seasonal patterns of CO_2 flux in boreal, temperate, and tropical forests in East Asia, Agric. Forest Meteorol., 148, 700–713, 2008.

Sampson, D. A., Janssens, I. A., Curiel Yuste , J., and Ceulemans, R.: Basal rates of soil respiration are correlated with photosynthesis in a mixed temperate forest, Glob. Change Biol., 13, 2008–2017, 2007.

Schwarz, P. A., Law, B. E., Williams, M., Irvine, J., Kurpius, M., and Moore, D.: Climatic versus biotic constraints on carbon and water fluxes in seasonally drought-affected ponderosa pine ecosystems, Global Biogeochem. Cy., 18, GB4007, doi: 10.1029/2004GB002234, 2004.

Scott, R. L., Jenerette, G. D., Potts, D. L., and Huxman, T. E.: The effect of drought on the water and carbon dioxide exchange of a woody-plant-encroached semiarid grassland, Agric. Forest Meteorol., in review, 2008.

Sellers, P. J., Mintz, Y., Sub, Y. C., and Dalcher, A.: A simple biosphere model (SiB) for use within general circulation models, J. Atmos. Sci., 43, 305–331, 1986.

Suyker, A. E. and Verma, S. B.: Year-round observations of the net ecosystem exchange of carbon dioxide in a native tallgrass prairie, Glob. Change Biol., 7, 279–289, 2001.

Takagi, K., Nomura, M., Ashiya, D., Takahashi, H., Sasa, K., Fujinuma, Y., Shibata, H., Akibayashi, Y., and Koike, T.: Dynamic carbon dioxide exchange through snowpack by wind-driven mass transfer in a conifer-broadleaf mixed forest in northernmost Japan, Global Biogeochem. Cy., 19, GB2012, doi: 10.1029/2004GB002272, 2005.

Thornley, J. H. M.: Instantaneous Canopy Photosynthesis: Analytical Expressions for Sun and Shade Leaves Based on Exponential Light Decay Down the Canopy and an Acclimated Non-rectangular Hyperbola for Leaf Photosynthesis, Ann. Bot.-London, 81, 451–458, 2002.

Tjoelker, M. G., Oleksyn, J., and Reich, P. B.: Modelling respiration of vegetation: evidence for a general temperature-dependent Q_{10}, Glob. Change Biol., 7, 223–230, 2001.

Vickers, D. and Mahrt, L.: The cospectral gap and turbulent flux calculations, J. Atmos. Ocean Tech., 20, 660–672, 2003.

Wang, C. K., Bond-Lambery, B., and Gower, S. T.: Carbon distribution of a well- and poorly-drained black spruce fire chronosequence, Glob. Change Biol., 9, 1066–1079, 2003.

Xu, L. and Baldocchi, D. D.: Seasonal variation in carbon dioxide exchange over a Mediterranean annual grassland in California, Agric. Forest Meteorol., 123, 79–96, 2004.

Yi, C. X., Davis, K. J., Berger, B. W., and Bakwin, P. S.: Long-term observations of the dynamics of the continental planetary boundary layer, J. Atmos. Sci., 58, 1288–1299, 2001.

Yuan, W., Liu, S., Zhou, G., Zhou, G., Tieszen, L. L., Baldocchi, D., Bernhofer, C., Gholz, H., Goldstein, A. H., Goulden, M. L., Hollinger, D. Y., Hu, Y., Law, B. E., Stoy, P. C., Vesala, T., and Wofsy, S. C.: Deriving a light use efficiency model from eddy covariance flux data for predicting daily gross primary production across biomes, Agric. Forest Meteorol., 143, 189–207, 2007.